ISSN 0010-9525, Cosmic Research, 2018, Vol. 56, No. 3, pp. 223–231. © Pleiades Publishing, Ltd., 2018.
Original Russian Text © V.A. Shuvalov, N.B. Gorev, N.A. Tokmak, G.S. Kochubei, 2018, published in Kosmicheskie Issledovaniya, 2018, Vol. 56, No. 3, pp. 243–250.

Physical Simulation of a Prolonged Plasma-Plume Exposure of a Space Debris Object

V. A. Shuvalov[a], *, N. B. Gorev[a], N. A. Tokmak[a], and G. S. Kochubei[a]

[a] *Institute of Technical Mechanics, National Academy of Sciences of Ukraine, Dnepropetrovsk, 49600 Ukraine*

**e-mail: vashuvalov@ukr.net*

Received June 9, 2016

Abstract—A methodology has been developed for the physical (laboratory) simulation of the prolonged exposure of a space debris object to high-energy ions of a plasma plume for removing the object into low-Earth orbit with its subsequent burning in the Earth's atmosphere. The methodology is based on the equivalence criteria of two modes of exposure (in the Earth's ionosphere and in the setup) and the procedure for accelerated resource tests in terms of the sputtering of the space debris material and its deceleration by a plasma jet in the Earth's ionosphere.

DOI: 10.1134/S0010952518020090

INTRODUCTION

The near-Earth space now contains more than 10000 space debris objects, i.e., fragments of rocket and space equipment, upper stages of carrier rockets, fuel tanks, expired spacecraft (SC), etc., which present a hazard for functioning SC. Recent years have seen an increase in project proposals to clean up the near-Earth space by removing space debris objects (SDOs) into low-Earth orbit (LEO) where they will subsequently be burnt in the dense layers of the Earth's atmosphere. One of these projects to clean up the near-Earth space by removing SDOs into LEO through deceleration induced by exposure to a plasma plume generated by an electric propulsion engine (EPE) or a plasma accelerator onboard another SC is LEOSWEEP (European Space Agency) [1, 2]. It is proposed to expose SDOs to Xe^+ ions of a plasma plume with an energy of ~1–5 keV [3]. The efficiency of the implementation of this project largely depends on the transfer of momentum of high-energy Xe^+ ions to the SDO surface material, i.e., screen-vacuum heat insulation (SVHI). At a distance of minimum safe approach of an SC to an SDO (≥7 m) [1–3], regardless of the type of EPE, the concentration of high-energy Xe^+ ions does not exceed 10^7 cm^{-3}. Therefore, when an SDO is deorbited from a 650-km orbit and lowered to, e.g., ~300 km, its exposure to high-energy Xe^+ ions may last as long as 100 days or more. A prolonged plasma-plume exposure of an SDO is characterized by the sputtering of the coating material and the transfer of momentum from high-velocity Xe^+ ions to the SDO. The coating of an SDO, e.g., third stage of the *Tsiklon 3* vehicle, is SVHI consisting of 10 layers of perforated aluminized mylar PET film with a thickness of 5×10^{-4} cm. The film is duplicated with KhSVN-7 fiberglass canvas, which protects the film layers from sticking together.

The SVHI coating is a mesh of E2-62 fiberglass fabric, i.e., a permeable surface with a continuous fiber thickness of $\sim 2.5 \times 10^{-2}$ cm. The fiberglass fabric is made of aluminoborosilicate continuous fiber. The fiber is composed of SiO_2 (54%), B_2O_3 (5%), Al_2O_3 (14%), CaO (23%), MgO (2.5%), Na_2O (0.5%), and other components with contents of less than 0.3% each. The bulk density of the fiber is $\rho_W \approx 2.5$ g/cm^3 and the average molecular mass is $m_W \approx 65.5$ amu. The SVHI is applied to the metal casing of the third stage of *Tsiklon 3* vehicle, i.e., to a sheet with a thickness of 1.0 cm or less, composed of an AM g-6M aluminum–magnesium alloy. There is so far no research on the interaction of Xe^+ ions with energies of $E_i \gg 10^2$ eV with SVHI. The complex composition, relief, and structure of SVHI render numerical simulation of this interaction virtually impossible. One can only predict the consequences of a prolonged plasma-plume exposure of an SDO using special procedures of physical simulation.

The aim of this work is to develop procedures and means of physically (laboratory) simulating of a prolonged plasma-plume exposure of SVHI in terms of the sputtering of the material and momentum transfer to the SDO.

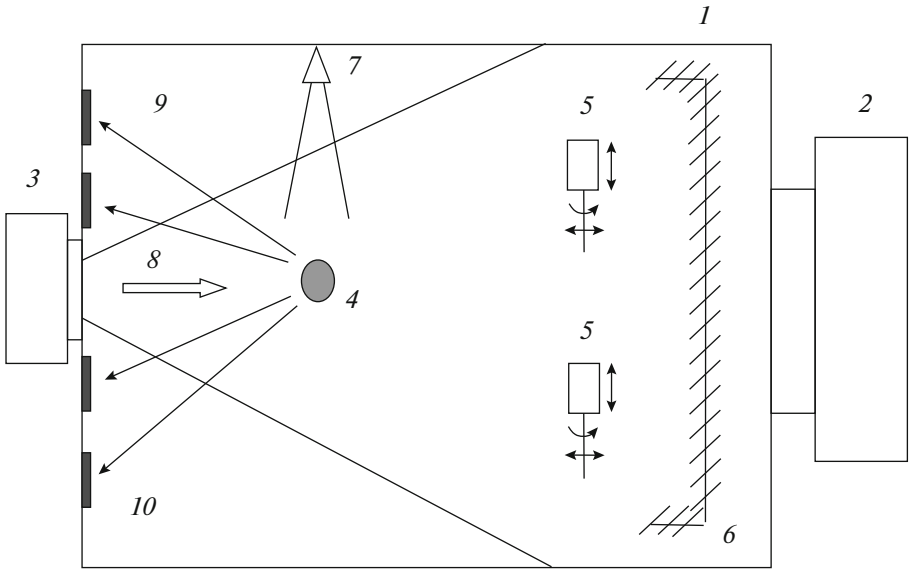

Fig. 1. Scheme of the experiments on SVHI sputtering with Xe^+ ions. (*1*) Vacuum chamber; (*2*) evacuation system; (*3*) generator of the rarefied plasma flux (plasma accelerator); (*4*) sample material (model, or fragment); (*5*) contact probe diagnostics system on the upper mobile platform with four degrees of freedom; (*6*) liquid nitrogen (LN_2) cooled cryopanels; (*7*) antenna of a microwave (5.45 GHz) interferometer; (*8*) incident plasma flux; (*9*) sputtered particles; (*10*) strips of mirror-polished metal foil to record the dispersion of the sputtered material.

SPUTTERING OF SDO COATING MATERIAL

Experimental Procedure

The experimental studies were carried out in the plasmodynamic setup of the Institute of Technical Mechanics (ITM). The setup belongs to the class of plasma gas-dynamic tunnels, designed to study the interaction of SC with the Earth's ionosphere by simulation and imitation [4–6]: the transfer of momentum and energy of rarefied plasma fluxes to the SC surface and systems (aerodynamics and heat exchange); electroradiation differential charging and neutralization of SC in geostationary orbits and in the polar ionosphere; and the physicochemical degradation of structural materials of SC outer surfaces. The scheme of the experiment is shown in Fig. 1.

The setup vacuum chamber (cylinder with diameter of 1.2 m and length of 3.5 m) is made of nonmagnetic stainless steel. The setup vacuuming system (mechanical pumps with capacity of up to 2.5 m^3/s; diffusion pumps with a pumping rate of ~50 m^3/s; and oil-free pumping with air capacity of ~50 m^3/s, i.e., a vacuum electric discharge unit and a turbomolecular pump), including the presence in the vacuum chamber of cryopanels cooled with liquid nitrogen LN_2, maintains in the working section a static rarefaction of ~10^{-5} N/m^2 and, given an inleakage of gas, a pressure of 10^{-3} N/m^2 [6].

Samples of materials being tested, fragments of structural elements, SC payloads, and setup diagnostic tools are placed on mobile platforms (upper and lower one) with four degrees of freedom each, which ensure longitudinal and transverse mobility the horizontal plane, mobility in the vertical plane, and rotation around a vertical axis. The reading accuracy is 0.5 mm for linear movements and 0.5° for angular movements. During the experiment, samples of the materials tested, SC models, and diagnostic probes can be moved to nearly any point of the plasma plume and the vacuum chamber volume. The parameters of the plasma fluxes are measured using a system of electric probes and a microwave interferometer operating at a frequency of 5.45 GHz [6]: cylindrical tungsten probes with radii of $r_p = 1 \times 10^{-2}$ cm and lengths of $l_p \approx 1.0$ cm and molybdenum probes with $r_p = 4.5 \times 10^{-3}$ cm and $l_p = 0.45$ cm; a spherical probe with a diameter of $2r_p = 0.40$ cm; a planar molybdenum probe with a diameter of $2r_p \approx 1.0$ cm; and a molybdenum Faraday cylinder with a diameter of $r_p \approx 1.0$ cm and height of $l_p \approx 1.0$ cm.

The energy E_i of the directed movement of the ion flux is controlled by an energy analyzer, a multielectrode probe. The spread of the measured E_i values does not exceed ±4.5%. The source of high-energy ions of rarefied plasma fluxes was a gas discharge accelerator whereby the working gas is ionized by an electron shock and electrons oscillate in the external magnetic field. Using the accelerator, one can generate supersonic fluxes of rarefied plasma (with H_2, He, Ne, N_2, O_2, Ar, Kr, and Xe^+ as working gases), obtain ion fluxes with energies of 0.1–0.3 keV and, given a multielectron sys-

tem for the additional acceleration of ions, we obtain Xe^+ fluxes with energies of 0.75–1.8 keV.

Current-voltage characteristics (CVCs) are recorded in automatic mode. The measurement error of the probe current does not exceed ±2%. The plasma potential was measured with respect to the point of divergence of the characteristics associated with the cold and heated thermal probe. The spread in the values of the plasma potential is no greater than ±4%. The orientation of the sample targets relative to the incident flux velocity vector was controlled using a single cylindrical probe of radius $r_p \approx 4.5 \times 10^{-3}$ cm and length $l_p \approx 0.45$ cm. The ionic current peak detected by the probe during the rotation around the horizontal axis corresponds to the orientation of the probe axis along the flux, and the halfwidth of the ionic current peak is proportional to the degree of nonisothermicity of the rarefied plasma. The composition of the residual gas in the setup vacuum chamber was controlled using an MX 7307 mass spectrometer [6, 7].

The sputter experiments used two samples, i.e., the SDO coating material (the SVHI sample) and 12Kh18N10T stainless steel (the STEEL sample). The SVHI sample was essentially an SVHI mat placed in an envelope of E2-62 fiberglass fabric. An AM g-6M aluminum–magnesium alloy sheet with a width of 1×10^{-1} cm was used as a substrate. The reliability and accuracy of the results obtained by testing the SVHI sample in an Xe^+ ion flux with an energy of $E_i \gg 10^2$ eV was checked using a control sample of 12Kh18N10T stainless steel with an irradiated surface that had the same area as that of the SVHI sample. The composition of 12Kh18N10T stainless steel includes: Fe (68%), Cr (18%), Ni (10%), Mn (2%), Si (0.8%), and C (0.12%). The bulk density of the steel is $\rho_W = 7.9$ g/cm^3; the average molecular mass is taken at $m_W = 55.2$ amu. The experiments used samples shaped as circular discs with outer diameters of $d_1 = 41 \times 10^{-1}$ cm and irradiated-surface diameter of $d_W = 33.5 \times 10^{-1}$ cm. The SVHI and STEEL samples were put onto the setup's lower mobile platform with four degrees of freedom in Xe^+ plasma fluxes with an ion energy from 0.2–1.8 keV and ion concentration of $n_i \approx 3.1 \times 10^8$ cm^{-3} at electron temperatures $T_e = 2.5$–3.0 eV and ion temperatures $T_i = 0.4$–0.7 eV. The time of sample exposure was $t = 2.0$ h.

The mass characteristics of the tested samples were measured outside the vacuum chamber before and after the flux exposure (with an interval of ~1 h before and after the vacuuming and plasma exposure) using an analytical microbalance with a measurement error of no more than 1×10^{-4} g. By weighing the samples outside the vacuum chamber with an interval of 1 h before and after the vacuuming and plasma exposure, we ensured identical conditions for mass determination of the irradiated material of the sample. The mass loss was $\delta M_W = M_1 - M_2$, where M_1 and M_2 are the masses of the sample before and after its exposure in the plasma flux and in vacuum. The contribution of adsorbed gases δM_a in air at atmospheric pressure before and after the vacuuming and after the plasma-flux irradiation was calculated as follows: $\delta M_W \approx (M_1 + \delta M_a) - (M_2 + \delta M_a)$.

Sputter Coefficients

When processing, analyzing, and interpreting the test results, we considered the conclusions and results obtained by studying the sputtering of materials during bombardment with ions of rarefied plasma fluxes as follows [8–15]:

(1) The sputter coefficients for rough surfaces are smaller than for smooth ones. This is because some of the atoms are captured by neighboring microirregularities.

(2) The energy spectrum of the sputtered particles is weakly dependent on the energy of the bombarding ions and, at $E_i \geq 1$ keV, remains almost unchanged. The average energy E_s of the sputtered particles is on the order of tens of electronvolts. Approximately 95–99% of the sputtered particles have energies of $E_s \approx 20$ eV [12, 13].

(3) For polycrystals, in the first approximation, the angular distribution of the sputtered particles given the normal incidence of bombarding ions with energies $E_i = 1$–10 keV conforms to the cosine law. For rough surfaces, the cosine distribution is almost independent of the angle of incidence [8, 9].

(4) At $0.7 < E_i < 70$ keV and $M_i > m_W$ (M_i is the ion mass and m_W is the mass of the particle of the sputtered material), the sputter coefficient Y_W is proportional to $E_i^{0.5}$. At velocities of bombarding ions of up to ~150 km/s, the Y_W coefficient and the sputter velocity are linearly dependent on the ion flux velocity U_i [10–12].

The sputter coefficients Y_W for the SVHI sample and the control STEEL sample during bombardment with rarefied plasma ions were determined by the formula

$$Y_W = \frac{e\delta M_W}{m_W I_{0i} t}, \quad (1)$$

where e is the electron charge, A s; I_{0i} is the ionic current on the surface of the sample given the normal incidence, A; and t is the exposure time, s.

The sputter velocity is

$$\bar{V}_W = \frac{Y_W m_W I_{0i}}{e\rho_W A_W} = \frac{\delta M_W}{\rho_W A_W t}, \quad (2)$$

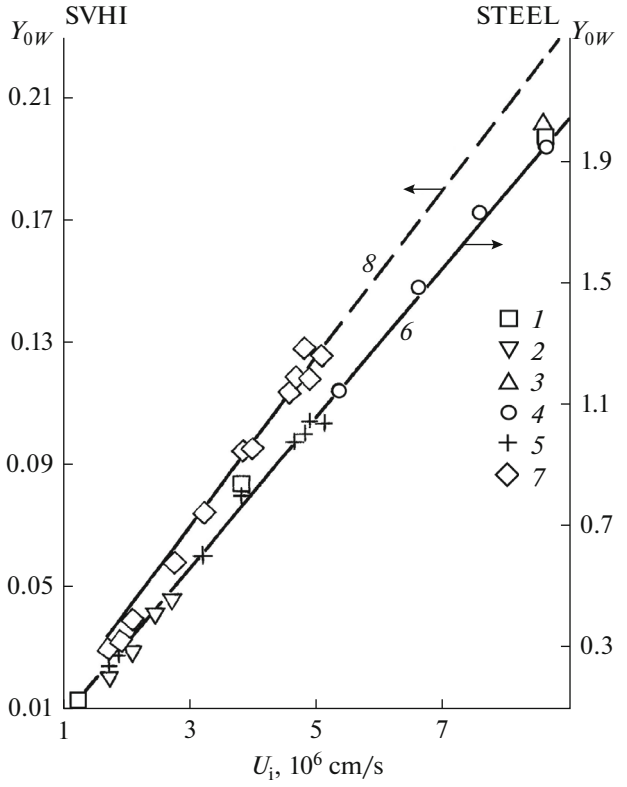

Fig. 2. Dependences of the sputter coefficients for the SVHI and STEEL samples on the velocity of bombarding Xe^+ ions at normal incidence ($\theta = 0°$). STEEL: (*1*) [14]; (*2*) [10]; (*3*) [15] for Kr^+; (*4*) [9]; (*5*) authors' measurements; (*6*) linear dependence $Y_{0W} \sim U_i$. SVHI: (*7*) authors' measurements; (*8*) linear dependence $Y_{0W} \sim U_i$; the dashed portion of line *8* is the approximation $Y_{0W_2} \approx Y_{0W_1}\left(U_{i2}/U_{i1}\right)$ for 5×10^6 cm/s $\le U_{i2} \le 8 \times 10^6$ cm/s.

where ρ_W is the density of the material, g/cm^3, and A_W is the area of the irradiated surface, cm^2.

In the plasma flux, when the SVHI sample is irradiated with Xe^+ ions with an energy of $E_i = 1.8$ keV, for $m_W = 65.5$ amu, $A_W = 8.81$ cm^2, $I_{0i} = 2.24 \times 10^{-3}$ A, $n_i = 3.1 \times 10^8$ cm^{-3}, $\rho_W = 2.54$ g/cm^3, $t = 7.2 \times 10^3$ s, and $\delta M_W = 1.43 \times 10^{-3}$ g given the normal incidence of ions ($\theta = 0°$), it follows from (1) that $Y_{0W} = 0.127 \pm 0.013$ at a mass-loss rate of $\delta^* M_W = \delta M_W / t = 2 \times 10^{-7}$ g/s. At $E_i = 1.8$ keV, the sputter velocity for the SVHI sample is $\bar{V}_W \approx 8.9 \times 10^{-2}$ nm/s and the bulk concentration of the sputtered particles [9] is $n_W = \dfrac{e\delta M_W n_i}{m_W Y_{0W} t} \approx 4.02 \times 10^7$ cm^{-3}. The dependences of the sputter coefficients for the SVHI and STEEL samples on the velocity U_i of the bombarding ions are shown in Fig. 2.

The outer surface of the SVHI sample is the permeable E2-62 fiberglass fabric. At $E_i \ge 1.5$ keV, the transparency coefficient of the fabric is $\delta_W \approx 0.2$. The mass loss of the E2-62 fabric at $E_i \approx 1.5$ keV was $\delta M_W \approx 1.13 \times 10^{-2}$ g, and the mass loss of the aluminized PET film (the first layer under the fabric) was $\delta M_W \approx 8.5 \times 10^{-4}$ g, i.e., δM_W(E2–62) $\gg$ δM_W(PET). The mass loss of the aluminized PET film is negligibly small compared to that of the fiberglass fabric, the SVHI coating. The tested SVHI and STEEL samples were synchronously irradiated in the setup with a flux of irradiated Xe^+ plasma (under the same experimental conditions). The same procedure was used in the analysis, processing, and interpretation of the measurements. The consistency of the measured sputter coefficient Y_{0W} for the STEEL sample with the data in [9, 10, 14, 15] is also indirect evidence of the validity of the Y_{0W} measurements for the SVHI sample.

Equivalence of the Exposure Modes in the Ionosphere and in the Setup

The exposure time for the samples in the setup in a flux of Xe^+ ions with an energy of $E_i = 1.8$ keV and concentration of $n_i = 3.1 \times 10^8$ cm^{-3} was $t = 2$ h. The condition for the equivalence of setup experiments with the operating conditions in the ionosphere can be derived from the thermodynamic (entropic) equivalence criterion for material loading during accelerated resource tests [6]. According to the entropic equivalence criterion, two exposure (loading) modes are equivalent if they cause in the material the same increments in the irreversible component of entropy. The condition for equivalence between setup and in situ plasma-flux exposures of materials, given the identical sort and the same velocity of the particles bombarding the surface, is the equality of the integral fluences of ions $F_{i_M} = F_{i_H}$, where the subscripts M and H indicate the setup experiment and in situ operating conditions in the ionosphere, respectively.

The equality of the integral fluences is in fact the equivalence condition for the two modes of material loading that allow one to determine the time t_H of the plasma-flux exposure of the SDO in the ionosphere, which is equivalent to the time t_M of irradiation in the setup as follows:

$$t_H = \frac{n_{i_M} U_{i_M}}{n_{i_H} U_{i_H}} t_M = \frac{n_{i_M}\sqrt{E_{i_M}}}{n_{i_H}\sqrt{E_{i_H}}} t_M. \qquad (3)$$

On the other hand, for the sputtering of material during bombardment with plasma ions, the equivalence condition for the two ion exposure modes can be the equality of the integral mass-loss values from a unit area of the irradiated surface

$$\frac{\delta_{M_W}}{m_W} = \frac{Y_{0W} j_{0\mathrm{i}} t}{e} = Y_{0W} n_{\mathrm{i}} U_{\mathrm{i}} t, \quad (4)$$

where $j_{0\mathrm{i}} = e n_{\mathrm{i}} U_{\mathrm{i}}$ is the density of the ionic current on the irradiated surface at $\theta = 0°$. Then,

$$t_H = \frac{Y_{0M} n_{\mathrm{i}_M} U_{\mathrm{i}_M}}{Y_{0_H} n_{\mathrm{i}_H} U_{i_H}} t_M = \frac{Y_{0M} n_{\mathrm{i}_M}}{Y_{0_H} n_{\mathrm{i}_H}} \sqrt{\frac{E_{\mathrm{i}M}}{E_{\mathrm{i}H}}} t_M. \quad (5)$$

Considering that at $1 \le E_{\mathrm{i}} \le 5$ keV, the condition $Y_{0_2} \approx Y_{0_1}(U_2/U_1)$ is satisfied, it follows from (5) that

$$t_H = \frac{n_{\mathrm{i}_M} E_{\mathrm{i}_M}}{n_{\mathrm{i}_H} E_{\mathrm{i}_H}} t_M. \quad (6)$$

At $E_{\mathrm{i}M} = E_{\mathrm{i}H}$, conditions (3) and (6) are equivalent.

It follows from (3) for the Xe^+ ion flux at a distance of ~10 m from the nozzle exit in the ionosphere [3] in the ESA LEOSWEEP project at $E_{\mathrm{i}_H} = 3.5$ keV, $n_{\mathrm{i}_H} = 3.3 \times 10^6$ cm^{-3}, $E_{\mathrm{i}_M} = 3.5$ keV, $n_{\mathrm{i}_M} = 3.1 \times 10^8$ cm^{-3}, and $t_M = 2$ h that $t_H = 188$ h.

For $E_{\mathrm{i}_H} = 3.5$ keV, $n_{\mathrm{i}_H} = 3.3 \times 10^6$ cm^{-3}, and the testing conditions at $E_{\mathrm{i}_M} = 1.8$ keV, $n_{\mathrm{i}_M} = 3.1 \times 10^8$ cm^{-3}, and $t_M = 2$ h, we derive from (6) that $t_H = 97$ h and, from (3), we have $t_H = 135$ h.

It should be noted that (3) is the equivalence condition for the two irradiation modes and (6) is the equivalence condition for sputter processes under two modes of irradiating the material with plasma-flux ions.

In LEO in the ionosphere, the surface temperature of SC structural elements varies from 150 K (nighttime) to 400 K (daytime). During the setup experiments with the SVHI and STEEL samples, the surface temperature of stainless steel from the thermocouple readings (chromel–copel) was $T_{W_M} \le 420$ K. The temperature of the thermocouple in the cell of the SVHI fiberglass fabric did not exceed 450 K. The density of the energy flux transported by Xe^+ ions in the setup is almost twice as high as that of the energy flux transported by Xe^+ ions in the LEOSWEEP project at ~10 m from the nozzle exit of the ionic engine. Unlike in the setup experiment, the Xe^+ ion flux in the ionosphere falls onto the surface of a nonstabilized (tumbling) SC. These circumstances lead us to assume that, when the SVHI and STEEL samples are irradiated with Xe^+ ions with energies of $E_{\mathrm{i}_H} = E_{\mathrm{i}_M}$, the surface temperature of the SDO material does not exceed that of the samples in the physical experiment, i.e., $T_{W_H} \le T_{W_M}$. Based on the data in [8, 15], at $T_W \le 700$ K, the sputter coefficients for clean metal surfaces (W, Ta, and Pt) irradiated with rarefied plasma ions with energies of $E_{\mathrm{i}} \approx 1.2$–$2.6$ keV do not depend on the temperature of the irradiated surface. Taking into account these data, the dependences $\gamma_W(U_{\mathrm{i}})$ obtained for the SVHI and STEEL samples correspond to the maximum values of the sputter coefficients under the conditions of irradiation of these materials with Xe^+ ions in the sunlit portions of the SC orbit in the Earth's ionosphere.

One of the most popular polymer SC coatings is kapton-H. There is little data on sputter coefficients for kapton-H with Xe^+ ions. If we assume that the sputter coefficient for kapton-H with Xe^+ ions with an energy of 0.5–5.0 keV follows the dependence $\gamma_{0W_2} = \gamma_{0W_1}(U_{\mathrm{i}_2}/U_{\mathrm{i}_1})$, then the measurement results in [16, 17] for the kapton–Xe^+ system, i.e., $\gamma_W = 0.0143$–0.0189 at $E_{\mathrm{i}} = 0.35$ keV and $\gamma_W = 0.0297$ at $E_{\mathrm{i}} = 0.5$ keV can be used to estimate the values of γ_W in the kapton–Xe^+ system at $E_{\mathrm{i}} \ge 1$ keV. As a result, for the kapton–Xe^+ system, we derive $\gamma_W \approx 0.043$–0.057 at $E_{\mathrm{i}} \approx 1.8$ keV.

The data in [16, 17] for the kapton–Xe^+ system at $E_{\mathrm{i}} = 0.35$ and 0.5 keV differ from the values of γ_W for SVHI–Xe^+ shown in Fig. 2 by a factor of 2–2.5, i.e., for SVHI at $E_{\mathrm{i}} = 0.35$ keV, $\gamma_W \approx 0.048$ and, at $E_{\mathrm{i}} = 0.5$ keV, $\gamma_{\mathrm{i}} \approx 0.060$.

Given the ratio $\gamma_W(\mathrm{SVHI})/\gamma_W(\mathrm{kapton}) \approx 2$–$2.5$, the values $\gamma_W = 0.127 \pm 0.013$, which were measured by the authors in the Xe^+ flux for SVHI at $E_{\mathrm{i}} = 1.8$ keV, must correspond to the values $0.051 \pm 0.05 \le \gamma_W \le 0.063 \pm 0.007$ in the kapton–Xe^+ system.

DYNAMIC IMPACT OF PLASMA-FLUX IONS ON THE SDO COATING MATERIAL

The efficiency of the removal of an SDO into LEO largely depends on the momentum transfer from Xe^+ ions to the SDO surface material. The force action of the plasma plume on the surface of a solid body can be estimated using momentum and energy transfer coefficients (accommodation coefficients). The latter coefficients are used in calculated relationships, regardless of the accepted scheme that describe the interaction of gas ions with the surface of a solid body.

Currently, the best-understood process of the interaction of gas atoms and ions with a surface is that, for the particle energy range of 1–100 eV. For energies of $E_{\mathrm{i}} \gg 10^2$ eV, the only well-studied mechanisms are those of interactions of gas ions with crystal structures. Most SC structural materials are alloys, composites, or polymers with a complex structure and surface relief, and SVHI is one of them. The effect of the rough surface in particle collisions with a solid body for attack angles θ close to a normal incidence manifests itself in diminished momentum transfer coeffi-

cients and, consequently, in the increased drag force (drag coefficient) [18, 19].

The force action of a supersonic flux of rarefied plasma on a nonconducting dielectric surface is determined by bombardment with ions, electrons, sputtered particles, and the Coulomb interaction. The effect of the plasma flux on the surface element of a solid body is determined by the integral force [20]

$$F_\Sigma = F_i + F_e + F_s + F_c, \quad (7)$$

where F_i is the pressure of plasma-flux ions on the surface of a solid body, F_e is the pressure of plasma-flux electrons, F_s is the reactive force due to surface sputtering, and F_c is the Coulomb force.

In the study of the dynamic interaction of Xe^+ ions with the SVHI sample, we used the technique and procedures in [20] and relations (8) for the transfer coefficients for normal σ_n and tangential σ_τ momenta

$$\sigma_n = \frac{1+\left[1-e\left(F_x+F_y\tan\theta\right)\Big/\sqrt{2M_iE_i}I_i\right]\Big/\sqrt{1+\eta^2\Big/\cos^2\theta)}}{1-\sqrt{\pi kT_W\left(1+\eta^2\right)\Big/4E_i\left(\cos^2\theta+\eta^2\right)}}, \quad (8a)$$

and

$$\sigma_\tau = \frac{e\left(F_x - F_y\cot\theta\right)}{\sqrt{2M_iE_i}I_i}, \quad (8b)$$

where F_x is the drag force of the target, F_y is the buoyant force of the target in the ion flux, θ is the attack angle of the target, I_i is the ionic current onto the surface of the target, $\eta^2 = e\varphi_W/E_i$, $\varphi_W = \varphi_p - \varphi_0$ is the target surface potential φ_p relative to the plasma potential φ_0, k is the Boltzmann coefficient, and T_W is the surface temperature of the target.

Experiment Procedure

The target, a flat SVHI plate, was placed on a microbalance with high immunity to interferences from electric and magnetic fields [4]. The sensitive element of this microbalance was a strain-gauge transducer. The signal from the strain–gauge transducer was proportional to the shoulder deformation due to the action of an external force. The measurement error for this force was no more than ±3%. The range of the measured forces was 10^{-6} to 10^{-1} N.

The local parameters of the plasma flux were controlled by probe diagnostic systems placed on the upper mobile platform [7]. The floating potential of the target is assumed to be equal to that of the stainless-steel target placed onto the upper mobile platform.

Ion–SVHI Target Momentum Transfer Coefficients

The results of studying the dynamic (force) interaction of Xe^+ ions with energies of 0.2–1.8 keV with the SVHI surface are shown in Figs. 3a and 3b.

The maximum drag force of the flat plate in the hypersonic flux of rarefied plasma corresponds to the conditions of normal incidence of Xe^+ ions ($\theta = 0°$). The integral drag force F_Σ (7) of the plate at $\theta = 0°$ includes several components [18, 20]. The pressure force of the ion flux onto the surface of a solid body is

$$F_i = \left(\rho_i U_i^2/2\right)A_W \times\left[2\left(2-\sigma_{0n}\right)\left(1+1/2S_i^2\right)+\sigma_{0n}\left(\sqrt{\pi}/S_W\right)\right], \quad (9)$$

where ρ_i and U_i are the density and velocity of ions in the plasma flux, $S_i = U_i/V_i$ is the velocity ratio of ions in the plasma flux, $V_i = \sqrt{2kT_i/M_i}$, $S_W = U_i/V_{T_W}$ is the velocity ratio of the reflected particles, $V_{T_W} = \sqrt{2kT_W/M_i}$, T_W is the surface temperature of the solid body, and A_W is the area of the irradiated surface of the solid body.

The pressure force of electrons in the rarefied plasma flux onto the target is

$$F_e = n_e k T_e A_W, \quad (10)$$

where n_e and T_e is the concentration and temperature of electrons in the plasma flux.

The Coulomb force of the flat plate with the hypersonic flux of rarefied plasma at $r_W/\lambda_d \geq 50$ is [20]

$$F_c = \left(\rho_i U_i^2/2\right) \times A_W\left[1-\exp\left(-\Phi_f^{0.5}/0.3\left(r_W/\lambda_d\right)\right)\right]\left(\sqrt{1+\eta^2}-1\right), \quad (11)$$

where r_W is the characteristic size of the body, λ_d is the Debye radius, $\Phi_f = |e\varphi_f|/kT_e$ is the dimensionless floating potential of the solid body in the plasma flux, $\varphi_f = \varphi_p - \varphi_0 = -\left(kT_e/e\right)\ln\left(\bar{V}_e/U_i\right)$ is the floating potential of the body surface φ_p relative to the plasma potential, $\bar{V}_e = \sqrt{8kT_e/\pi m_e}$ is the average velocity of electrons, and m_e is the electron mass.

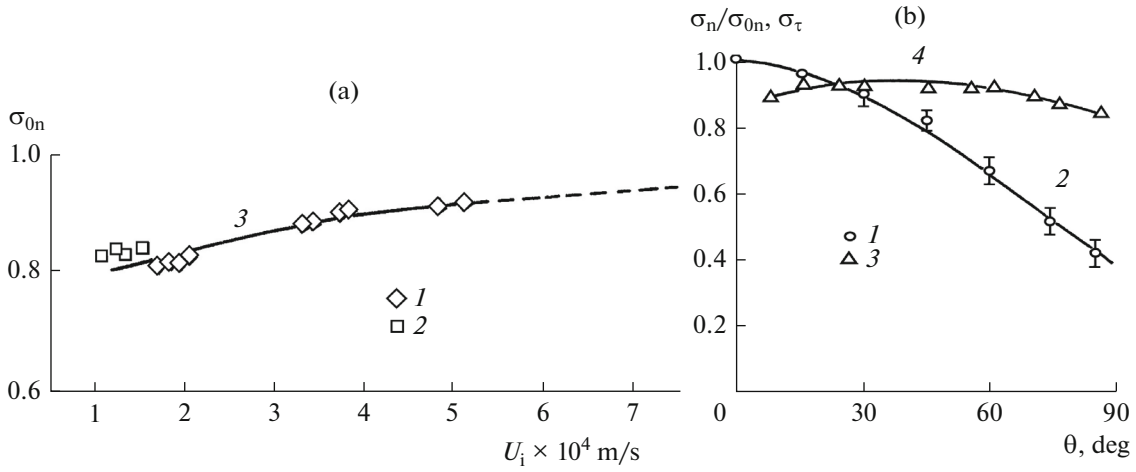

Fig. 3. (a) Dependence of the normal momentum transfer coefficient on the velocity of Xe^+ ions at $\theta = 0°$. (*1*) Authors' measurements and calculations using formula (8a); (*2*) data [20]; (*3*) averaging dependence (dashed line: extrapolation for $E_i > 1.8$ keV).

(b) Angular dependence of the coefficients of transfer of the normal $\sigma_n(\theta)/\sigma_{0n}$ and tangential $\sigma_\tau(\theta)$ momenta of Xe^+ ions to the SVHI surface at $E_i = 1.8$ keV. (*1*) Authors' measurements of $\sigma_n(\theta)/\sigma_{0n}$; (*2*) approximation $\sigma_n(\theta)/\sigma_{0n} = \cos^{3/2}\theta + 0.835(1 + 1/\sigma_{0n})^{-1}\sin\theta$ (dashes show the spread of values $\sigma_n(\theta)/\sigma_{0n}$ for the approximation); (*3*) authors' measurements of $\sigma_\tau(\theta)$; (*4*) averaging curve.

The pressure of sputtered particles onto the irradiated surface is

$$F_s = \left(\rho_s U_s^2/2\right) A_W \left[2\left(1 + 1/2S_s^2\right)\right], \qquad (12)$$

where ρ_s and U_s are the density and velocity of sputtered particles and $S_s = U_s/\sqrt{2kT_W/m_W}$ is the velocity ratio.

The parameters of the rarefied Xe^+ plasma flux in the ITM setup experiments are presented in Table 1.

The drag force components of the plate in the hypersonic flux of rarefied plasma at $\theta = 0°$, $E_i = 1.8$ keV, and $\sigma_{0n} \approx 0.92$ are given in Table 2. The decisive contribution to the dynamic interaction comes from Xe^+ ions bombarding the SVHI surface; the contributions from the other components can be ignored.

Equivalence of the Modes of Dynamic Impact of Plasma Ions on a Solid Body

Given the normal incidence ($\theta = 0°$) of ions in a hypersonic $S_i \gg 1$ flux of rarefied plasma onto a flat plate, from (8a) and (9), we derive the drag coefficient

$$c_x = \frac{F_x}{I_i U_i}\left(\frac{2e}{M_i}\right) = 2\left(2 - \sigma_{0n}\right). \qquad (13)$$

The magnitude of the c_x coefficient of the drag force F_x for a flat plate in a hypersonic $S_i \gg 1$ flux of rarefied plasma can serve as an equivalence criterion, i.e., a condition relating Mode 1 of dynamic interaction of SVHI with Xe^+ ions in orbit in the Earth's

Table 1. Plasma flux parameters

Flux parameters	E, keV	U, cm/s	V, cm/s	T, K	S	n, cm^{-3}	T_W	V_{T_W}	S_W	σ_{0n}	Y_{0W}	Φ_f
Ions (i)	1.8	5.13×10^6	9.4×10^4	7×10^3	5.46×10^1	3.1×10^8	5×10^2	2.51×10^4	2.04×10^2	0.92		
Electrons (e)	0.003			3.5×10^4		3.1×10^8	5×10^2					10
Sputtered particles (s)	0.02	7.65×10^5			3.05×10^1		5×10^2				0.13	

$S_i = U_i/V_i$; $S_W = U_i/V_{T_W}$; $A_W \approx 36$; $\lambda_d \approx 7.33 \times 10^{-2}$ cm; $r_W/\lambda_d \approx 81.9$; $\eta^2 = e\varphi_f/E_i \approx 1.6 \times 10^{-2}$

Table 2. Forces acting on the target in the rarefied plasma plume

n_i, cm^{-3}	F_i, N	F_e, N	F_c, N	F_s, N
3.1×10^8	6.95×10^{-4}	5.40×10^{-6}	3.34×10^{-7}	9.5×10^{-7}

atmosphere with Mode 2 of irradiation of the SVHI target with an Xe^+ ions flux in the setup

$$F_x = 2\left(2 - \sigma_{E_i}\right) n_i E_i A_W = \left(2 - \sigma_{E_i}\right) I_i U_i / e. \quad (14)$$

For the two modes of the material–plasma ion flux interaction,

$$F_{x1} = F_{x2}\left(\frac{2-\sigma_1}{2-\sigma_2}\right)\frac{n_{i1}E_{i1}A_{W1}}{n_{i2}E_{i2}A_{W2}} = F_{x2}\left(\frac{2-\sigma_1}{2-\sigma_2}\right)\frac{I_{i1}U_{i1}}{I_{i2}U_{i2}}, \quad (15)$$

where subscript 1 corresponds to the conditions of dynamic interaction in the Earth's ionosphere, subscript 2 indicates the conditions of interactions in the setup, and $\sigma_{1,2}$ corresponds to the conditions of normal ($\theta = 0°$) irradiation as follows: $\sigma_{1,2} = \sigma_{0n}\left(E_{i1,2}\right)$ or $\sigma_{1,2} = \sigma_{0n}\left(U_{i1,2}\right)$ (Fig. 3a).

Based on the numerical simulation of the plasma plume generated by an onboard electric propulsion engine in the ionosphere in the LEOSWEEP project, the average concentration of Xe^+ ions with an energy $E_{i1} = 3.5$ keV at a distance of ~7.0 m from the nozzle exit is $n_{i1} \approx 6.94 \times 10^6$ cm^{-3} and the irradiated area of the SDO surface is $A_{W1} = 4.15 \times 10^4$ cm^2 [3].

According to (15), for the SVHI target, it follows from the results of the setup experiments at $n_{i2} = 3.1 \times 10^8$ cm^{-3}, $E_{i2} = 1.8$ keV, $\sigma_2 = 0.92$, $A_{W2} = 36$ cm^2, $F_{x2} \approx 7 \times 10^{-4}$ N and $\sigma_1 = 0.94$ at $E_{i1} = 3.5$ keV (Fig. 3a) that $F_{x1} \approx 35 \times 10^{-3}$ N. For a fully diffuse scheme of dynamic interaction of Xe^+ ions with the target material at $\sigma_1 = \sigma_2 = 1.0$ and $F_{x2} \approx 6.4 \times 10^{-4}$ N, according to (9), it follows from (15) that $F_{x1} \approx 32 \times 10^{-3}$ N (with an error of no more than 3.5%).

CONCLUSIONS

We developed procedures and technical means for physical (laboratory) simulation of a prolonged exposure of the coating material of a space debris object to high-energy ($E_i \gg 10^2$ eV) ions in a rarefied plasma flux generated by an onboard electric propulsion engine in terms of sputtering of the material and the transfer of momentum from gas ions. Based on the experiments, we derived dependences of the sputter coefficients for the coating material of the space debris objects (screen vacuum heat insulation) and the accommodation coefficients for the normal and tangential momenta of high-energy Xe^+ ions onto screen vacuum heat insulation on the energy of the bombarding particles. We derived relationships for establishing the consistency between the procedure of the accelerated setup experiments and the conditions of a prolonged plasma-plume exposure of a space debris object in the Earth's ionosphere.

ACKNOWLEDGMENTS

This work was supported in part by the LEOSWEEP project, European Space Agency.

REFERENCES

1. Bombardelli, C. and Peláez, J., Ion beam shepherd for contactless space debris removal, *J. Guid. Dyn.*, 2011, vol. 34, no. 3, pp. 916–920.
2. Kitamura, S., Hayakawa, Y., and Kawamoto, S., A reorbiter for GEO large space debris using ion beam irradiation, in *The 32nd International Electric Propulsion Conference*, Wiesbaden, Germany, 2011, 087, p. 10.
3. Merino, M., Ahedo, E., Bombardelli, C., Urrutxua, H., and Peláez, J., Hypersonic plasma plume expansion in space, in *The 32nd International Electric Propulsion Conference*, Wiesbaden, Germany, 2011, 08, p. 14.
4. Shuvalov, V.A., Tokmak, N.A., Pis'mennyi, N.I., and Kochubei, G.S., Dynamic interaction of a magnetized solid body with a rarefied plasma flow, *J. Appl. Mech. Tech. Phys.*, 2016, vol. 57, no. 1, pp. 145–152.
5. Shuvalov, V.A., Kochubei, G.S., Priimak, A.I., Gubin, V.V., and Tokmak, N.A., Radiation electrization of spacecraft leeward surfaces by auroral electrons in the ionosphere, *Cosmic Res.*, 2003, vol. 41, no. 4, pp. 413–423.
6. Shuvalov, V.A., Pis'mennyi, N.I., Kochubei, G.S., and Tokmak, N.A., The mass loss of spacecraft polyimide films under the action of atomic oxygen and vacuum ultraviolet radiation, *Cosmic Res.*, 2014, vol. 52, no. 2, pp. 99–105. doi 10.1134/S0010952514020063
7. Shuvalov, V.A., Pis'mennyi, N.I., Lasuchenkov, D.N., and Kochubei, G.S., Probe diagnostics of laboratory and ionospheric rarefied plasma flows, *Instrum. Exp. Tech.*, 2013, vol. 56, no. 4, pp. 459–467. doi 10.1134/S002044121304009X
8. Kaminskii, M., *Atomnye i ionnye stolknoveniya na poverkhnosti metalla* (Atomic and Ionic Impact Phenomena on Metal Surfaces), Moscow: Mir, 1967.
9. *Sputtering by Particle Bombardment*, Behrisch, R., Ed., Berlin: Springer, 1981; Moscow: Mir, 1986.
10. Pleshivtsev, N.V., *Katodnoe raspylenie* (Cathode Sputtering), Moscow: Atomizdat, 1968.
11. Ivanovskii, G.F. and Petrov, V.I., *Ionno-plazmennaya obrabotka materialov* (Ion–Plasma Processing of Materials), Moscow: Radio i svyaz', 1986.
12. Danilin, B.S., *Primenenie nizkotemperaturnoi plazmy dlya naneseniya tonkikh plenok* (Low-Temperature Plasma for Thin Film Deposition), Moscow: Energoatomizdat. 1989.

13. Ryzhov, Yu.A., Interaction of high-velocity rarefied flow with solid body surface, in *Problemy mekhaniki i teploobmena v kosmicheskoi tekhnike* (Problems of Mechanics and Heat Exchange in Space Technology), Belotserkovskii, O.M., Ed., Moscow: Mashinostroenie, 1982.

14. Belan, N.V., Kim, V.P., Oranskii, A.I., and Tikhonov, V.B., *Statsionarnye plazmennye dvigateli* (Stationary Plasma Engines), Khar'kov: Khar. aviats. inst., 1989.

15. Arifov, U.A., *Vzaimodeistvie atomnykh chastits s poverkhnost'yu tverdogo tela* (Interaction of Atomic Particles with Solid Body Surface), Moscow: Nauka. 1968.

16. Yalin, A.P., Surla, V., Faruell, C., Butweiller, M., and Williams, J.D., Sputtering studies of multi-component materials by weight loss and cavity ring-down spectroscopy, in *The 42nd AJAA/ASME/SAE/ASEE Joint Propulsion Conference*, Sacramento: AJAA, 2006, p. 4338.

17. Yalin, A.P., Rubin, B., Domingue, S.R., Glueckert, Z., and Williams, J.D., Differential sputter yields on boron nitride, quartz and kapton due to low energy Xe^+ bombardment, in *The 43rd AJAA/ASME/SAE/ASEE Joint Propulsion Conference and Exhibit*, Cincinnati: AJAA, 2007, p. 5314.

18. Barentsev, R.G., *Vzaimodeistvie razrezhennykh gazov s obtekaemymi poverkhnostyami* (Interaction of Rarefied Gases with Streamlined Surfaces), Moscow: Nauka, 1975.

19. Erofeev, A.I., The influence of roughness on the gas flow interaction with solid body surface, *Mekh. Zhidk. Gaza*, 1967, no. 6, pp. 82–89.

20. Shuvalov, V.A., *Modelirovanie vzaimodeistviya tel s ionosferoi* (Modeling the Interaction of Bodies with the Ionosphere), Kiev: Naukova dumka, 1995.

Translated by A. Kobkova